Surface Wave Propagation in Shallow Water beneath an Inhomogeneous Ice Cover

A. V. MARCHENKO AND K. I. VOLIAK

General Physics Institute, Russian Academy of Sciences, Moscow, Russia

(Manuscript received 28 March 1996, in final form 10 December 1996)

ABSTRACT

The scattering of flexural–gravity waves in a layer of shallow fluid beneath an ice cover with irregularities is investigated. The irregularities considered are the ice edges, cracks, areas of finely broken ice, and ice ridges. Even this idealized problem formulation demonstrates that the accumulated effect of a large number of irregularities may lead to complete dissipation of the energy of wind waves and swells. The analysis shows a strong scattering of such waves by periodic linear irregularities in the sea ice cover. The authors employ the shallow-water approximation, which makes the results applicable for ocean shelf areas.

1. Introduction

A large portion of the ocean's wave energy is carried by the waves that either are influenced by wind or have emerged from wind action areas—called wind waves and swell, respectively. According to the data of the USSR Register on the wave climate in Russian Arctic seas (see Smirnov 1987), typical periods of wind waves and swell lie in the range from 7.6 to 14 s. Experimental data on the spectral composition of flexural–gravity waves in the Arctic were analyzed by Nagurny et al. (1994) and Wadhams et al. (1995) to show that a major portion of the wave energy corresponds to waves with periods greater than 16 s. Wadhams et al. suppose that the most intensive vibrations of the ice cover are forced by the low-frequency portion of the swell spectrum, which propagates across long distances under the ice. Let us consider a surface wave source to be in open water. The waves propagating from such a source to the marginal zone of drifting ice, scatter partially there, and then propagate under the sea ice to a large distance. Sea ice is strongly inhomogeneous in composition and properties. The marginal ice zone consists of alternating regions of dense and sparse ice. The former often produce bands oriented along the wind direction. Cracks, polynias, and hummocks are the characteristic irregularities of dense ice, which can scatter the surface waves. In the study of surface wave propagation, the ice cover is conventionally modeled by a thin elastic plate. The waves in it are referred to as flexural–gravity ones on the assumption that the particle motion in them is governed by gravity, particle inertia, and surface tension acting upon water from the deformed ice cover. The main approximations of this model are the following: the wave's amplitude is small compared to its length; the plate thickness is small related to its curvature radius; and the ice elasticity greatly exceeds its viscosity, relaxation, and plasticity. The model is valid for waves of lengths greater than 100 m and amplitudes less than a few meters.

The model of a thin elastic plate does not include the floe's undulation about its center of mass, which is induced by waves. Spectral properties of the surface waves traveling in the dispersed ice cover, which consisted of isolated floes (rigid cylindrical discs), were studied by Masson and LeBlond (1989) who accounted for all degrees of freedom for each floe. At a sufficient ice cover density, the undulating floes touch each other. The modeling of ice collision and dispersion was considered by many authors [see the review by Squire et al. (1995)].

Pure linear inhomogeneities are the simplest in an elastic cover and are exemplified by a straight ice edge, a crack joining the edges of two floes, and a hummock ridge. The latter should have a width much shorter than its length and the length of incident flexural–gravity waves. Actually, these simple irregularities are rarely observed in nature, but they are very important as model examples.

Kouzov (1963) applied the Wiener–Hopf method to consider the hydroacoustic wave diffraction at a crack in an elastic plate floating on the surface of an infinitely deep fluid. The exact solution to that problem allowed him to calculate the coefficients of wave reflection and transmission, as well as the properties of scattered waves. Evans and Davies (1968) used the above technique to solve exactly the linear problem on surface wave diffraction at the edge of a floating elastic plate.

Corresponding author address: Prof. Konstantin I. Voliak, General Physics Institute, Russian Academy of Sciences, ul. Vavilova 38, Moscow 117942, Russia.
E-mail: voliak@koi.gpi.ru

Meylan and Squire (1994) and Fox and Squire (1994) analyzed numerically, minimizing a functional, the diffraction of a plane surface wave at one and two parallel ice bands and the oblique incidence of the wave onto a straight edge of an ice plate floating on the surface of a finite-depth fluid, respectively. The review by Squire et al. (1995) contains a vast bibliography on wave scattering in ice cover.

Marchenko (1994) proposed a method to solve the spectral problem of periodic vibrations in an elastic ice cover with an infinite number of cracks floating on the shallow water surface. The spectral properties of waves propagating in such a system were studied by Marchenko et al. (1995) to show damping gaps in the wave frequency spectrum: if the wave frequency matches the gap, the wave decays exponentially when traveling beneath the ice.

We support the above idea of Nagurny et al. (1994) and Wadhams et al. (1995) on a long-range propagation of low-frequency waves under the ice. The primary goal of the present paper is to investigate the scattering (diffraction) of flexural–gravity waves at different frequencies by typical irregularities of the sea ice cover—that is, cracks, hummocks, and areas of broken ice. On the basis of these simple examples, we try to demonstrate that swell energy can be greatly scattered by a large number of such irregularities. The main emphasis is made on the dependence of wave reflection and transmission on the number of irregularities in the ice cover.

2. Basic equations

We use the shallow water approximation to describe the wave motion in the system fluid–ice cover. Therefore, we will study the propagation of flexural–gravity waves with typical lengths $2\pi/k$ exceeding the fluid depth H. Formally the shallow-water equations result from the substitution of factor $\tanh(kH)$ by kH in the dispersion relation. Actually, since $1 - \tanh 1 \approx 0.2$, one can take the condition $kH < 1$, where k is a characteristic wave vector, as a criterion of the relevant approximation. Then in the one-dimensional case the linear equations for shallow water beneath an elastic plate are written as

$$\frac{\partial \eta}{\partial t} + H\frac{\partial^2 \varphi}{\partial x^2} = 0, \qquad \frac{\partial \varphi}{\partial t} + g\eta + \frac{D}{\rho}\frac{\partial^4 \eta}{\partial x^4} = 0. \quad (2.1)$$

Here φ is the velocity potential on the fluid surface; x and t are the horizontal coordinate and the time; η is the fluid surface elevation over the horizontal position of equilibrium; E, ν, and h are the ice plate's Young module, Poisson's ratio, and thickness, respectively; ρ is the fluid density; and

$$D = \frac{Eh^3}{12(1 - \nu^2)}$$

is referred to as the plate's rigidity on bending. For sea ice the following parameters are typical (Bogorodsky and Gavrilo 1980):

$$E = 10^9 - 10^{10}\ \mathrm{N\ m^{-2}}, \qquad h = 1 - 3\ \mathrm{m},$$
$$\nu = 0.3 - 0.4. \quad (2.2)$$

Modeling the ice cover by a thin elastic plate imposes additional limitations upon the scale of wave processes governed by (2.1). The relevant theory is valid for (i) plates of small thickness, related to the characteristic radius of curvature of the middle surface on bending and (ii) the plate vibrations of a small amplitude compared to the characteristic horizontal scale. The first is equivalent to $kh \ll 1$, which follows from the shallow water criterion $kH < 1$ and the evident approximation $h \ll H$. Condition (ii) in our case means simply that the amplitude of a flexural–gravity wave is small compared to its length; that is, (ii) corresponds to the accepted approximation of linear waves.

Equations (2.1) do not include the inertial motion of ice, negligible as compared to that of moving fluid in virtue of the above $h \ll H$ at close densities of ice and water.

The energy conservation law for plane linear waves (of small amplitude and independent of the horizontal y coordinate normal to x), that is, the integral of (2.1), is written as

$$\frac{\partial Q}{\partial t} = \frac{\partial \Pi}{\partial x}, \qquad Q = E_p + E_k + E_f, \quad (2.3)$$

where $Q dxdy$ is the total energy of a cylindrical fluid volume and a part of the elastic plate over the base $dxdy$ and Π is the energy flux in the system fluid-elastic plate. Therefore, Q includes the densities E_k and E_p of the fluid kinetic and potential energies and E_f of the elastic plate free energy

$$2E_p = \rho g \eta^2, \qquad 2E_k = \rho H\left(\frac{\partial \varphi}{\partial x}\right)^2,$$
$$2E_f = D\left(\frac{\partial^2 \eta}{\partial x^2}\right)^2, \quad (2.4)$$

while Π is given by

$$\Pi = \rho H \frac{\partial \varphi}{\partial x}\frac{\partial \varphi}{\partial t} + D\left(\frac{\partial^2 \eta}{\partial x^2}\frac{\partial^2 \eta}{\partial t \partial x} - \frac{\partial^3 \eta}{\partial x^3}\frac{\partial \eta}{\partial t}\right). \quad (2.5)$$

Equations (2.1) have the simple solution oscillating in the system at a constant frequency ω

$$\eta = a \exp[i(\omega t + kx)] + \text{c.c.},$$
$$\varphi = \frac{i\omega a}{k^2 H} \exp[i(\omega t + kx)] + \text{c.c.}, \quad (2.6)$$

where

$$\omega = \omega(k), \qquad \omega(k)^2 = k^2 H(g + Dk^4). \quad (2.7)$$

At any real ω, dispersion equation (2.7) has two real $\pm k_0$ and four complex conjugate $\pm k_e$, $\pm k_e^*$ roots, for definiteness $k_0 > 0$, $\Re k_e > 0$, and $Tk_e > 0$. For $k = \pm k_0$, solution (2.6) presents real periodic flexural–gravity waves traveling along the x axis. The complex roots are due to the elastic plate on the fluid surface and correspond to complex waves with an amplitude exponentially growing in one direction of the x axis or decaying in the opposite direction. In the absence of the plate, that is, as $D \to 0$, the complex waves vanish with $|k_e| \to \infty$, while the real root k_0 remains finite.

Let us calculate the energy density and flux for waves (2.6)

$$Q = \frac{\omega a^2}{Hk^2} e^{2i\theta} + \text{c.c.} + \frac{1}{2}\left[\frac{\omega^2}{H(kk^*)^2}(k + k^*)^2 - \frac{D}{\rho}(k^2 - (k^*)^2)^2\right] aa^* e^{i(\theta-\theta^*)},$$

$$\Pi = \frac{\omega^2 a^2}{Hk^3} e^{2i\theta} + \text{c.c.} + \omega(k + k^*) \times \left[\frac{\omega^2}{H(kk^*)^2} + \frac{D}{\rho}(k^2 + (k^*)^2)\right] aa^* e^{i(\theta-\theta^*)},$$

$$\theta = kx + \omega t. \quad (2.8)$$

After averaging (2.8) for real k over the wave period $2\pi/\omega$, we find

$$\langle \Pi \rangle = c_0 \langle Q \rangle, \qquad \langle Q \rangle = \frac{2\omega^2}{Hk^2} aa^*,$$

$$c_0 = \frac{\partial \omega}{\partial k}, \qquad k = \pm k_0, \quad (2.9)$$

where the angular brackets mean the relevant averages. One sees that real waves transfer energy at group velocity c_0. It also follows from (2.9) that in the case of two waves of equal energy in fluid of the same depth, the wave propagating beneath ice of smaller thickness should have larger amplitude.

Similar averaging for complex waves yields

$$\langle \Pi \rangle = 0,$$

$$\langle Q \rangle = \frac{1}{2}\left[\frac{\omega^2}{H(kk^*)^2}(k + k^*)^2 - \frac{D}{\rho}(k^2 - (k^*)^2)\right] aa^* e^{i(\theta-\theta^*)}. \quad (2.10)$$

Thus, in spite of energy loss in production of complex waves, they do not transfer energy, which also follows from decay of the waves along an x direction with no energy accumulation in any limited fluid volume.

We shall assume that the ice plate is inhomogeneous and discontinuous. The irregularities considered are cracks and hummock ridges. The discontinuities in the ice cover are areas of open water or finely broken ice whose elastic properties may be disregarded for the wave propagation. All irregularities are supposed to be one-dimensional to vary the ice properties only along the x axis. The basic irregular elements affecting the ice cover properties are shown in Fig. 1. Case a in Fig. 1 corresponds to free edges of the ice floes. In case b the edges are elastically hinged to the hummock ridge modeled by a concentrated mass. We assume the ridge to be previously formed by ice compression, which is absent at the moment.

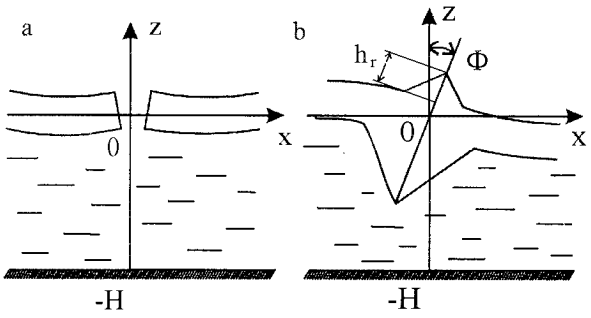

FIG. 1. Schematics of (a) the ice crack with free edges and (b) the ice hummock ridge.

An additional scale, that is, typical size of an irregularity, arises in the problem of inhomogeneous ice cover. Therefore, we consider the y length of the irregularity to be much longer than its x width. This width is also much less than the length of flexural–gravity waves. In general, short-wave (compared to the irregularity's width) perturbations can be produced by diffraction of a long wave. But in the model of a thin elastic plate we suppose that only negligible energy of long waves scatter into short waves and the scattering irregularity is purely linear (with no width). Such an approach allows us to model the irregularities by additional boundary conditions between contacting inhomogeneous floes.

To each type of irregularity correspond certain contact-boundary conditions to relate edge displacements, shear forces, and bending moments. The shear force F_x and bending moment M_{xx} are given by

$$F_x = -D\frac{\partial^3 \eta}{\partial x^3}, \qquad M_{xx} = -D\frac{\partial^2 \eta}{\partial x^2}. \quad (2.11)$$

The curved arrows in Fig. 2 show the positive direction of the bending moments that act on the floe edges AB and CD. The straight arrows show the positive direction of shear forces.

On a free plate edge the contact-boundary conditions are

$$M_{xx} = 0, \quad F_x = 0. \quad (2.12)$$

The hummock ridge is modeled by a thin inertial rigid rod frozen into the ice cover along the line $x = 0$, $z = 0$

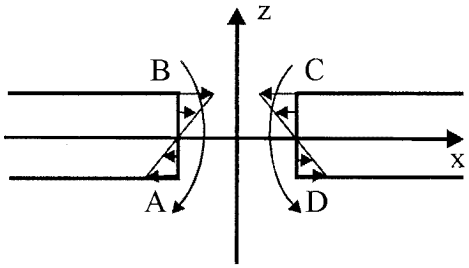

FIG. 2. Curvilinear arrows show the positive direction of bending moments acting on edges AB and CD of the ice plate. Horizontal arrows indicate stress directions in the plate.

(Marchenko 1994, 1995). A cross section of the rod consists of two triangles fixed by their bases to lower and upper surfaces of the plate (see Fig. 1b). The hummock's open height (''sail'') is about three times less than the thickness of its underwater part so that the hummock is statically balanced. The sloping angles of both the open and underwater parts are assumed to lie in the range from 30° through 45°. This presentation is in agreement with actual hummock structures (see, e.g., Zubov 1943). Coefficients in the equations of the rod motion depend on the mass m of unit length and the moment of inertia I related to the line $x = 0$, $z = 0$ in the absence of strain. Marchenko (1994) proposed for these parameters the estimates

$$m = \rho_i h_r(9.5h_r + 2h),$$
$$I = 2\rho_i h_r^3\,(7h_r + 0.3h), \tag{2.13}$$

where h_r is the sail of hummock and ρ_i is the ice density.

Torsion of the hummock is related to rotating the rod's vertical cross sections about the axis, while the bending is due to the axis curvature. We assume the hummock to hinge elastically to floe edges so that the bending moment is proportional to the variation in angle Φ (see Fig. 1b). In the one-dimensional case, there is no torsion and bending because the problem does not depend on the coordinate parallel to the hummock axis. In the absence of strain, the hummock is actually a concentrated mass with inertia related to vertical displacement and rotation about the y axis.

The contact-boundary conditions at the straight hummock ridge extended along y are given by Marchenko (1994):

$$m\frac{d^2\eta_0}{dt^2} = -\lim_{x\to-0} F_x + \lim_{x\to+0} F_x, \qquad \lim_{x\to\pm0} \eta = \eta_0,$$
$$I\frac{d^2\Phi}{dt^2} = -\lim_{x\to-0} M_{xx} + \lim_{x\to+0} M_{xx},$$
$$\lim_{x\to\pm0} M_{xx} = \mp\alpha\left(\lim_{x\to\pm0}\frac{\partial\eta}{\partial x} + \Phi\right), \tag{2.14}$$

where the angle Φ of hummock rotation is counted from the vertical. We choose $\Phi > 0$ for clockwise rotation. The factor α corresponds to the rigidity of hinges fixing the hummock to the ice edges.

In each vertical cross section of the fluid layer considered, the conservation laws should hold for mass and momentum:

$$[\varphi] = 0, \qquad \left[\frac{\partial\varphi}{\partial x}\right] = 0, \tag{2.15}$$

where the brackets show a jump of functions at certain x.

3. Wave diffraction at a crack and a hummock

Let us consider the diffraction of plane waves at an irregularity changing the thickness of ice cover by a jump. Parameters of the cover in regions $x > 0$ and $x < 0$ are denoted by subscripts 1 and 2. We introduce dimensionless coordinates, denoting them by primed letters (the primes will be omitted hereafter):

$$Tt' = t, \qquad lx' = x, \qquad T^2 = \frac{l^2}{gH},$$
$$l^4 = \frac{Eh_1^3}{12\rho g(1-\nu^2)}. \tag{3.1}$$

This normalization with clear physical meaning reduces the number of parameters of the initially stated problem. Therefore, the value of l does not obligatorily exceed much the fluid depth H.

Eliminating the elevation η in (2.1), passing to the dimensionless variables (3.1), and assuming the solution to be dependent on time t via the factor $\exp(i\gamma t)$, we find

$$\gamma^2\varphi + \left(1 + \frac{\partial^4}{\partial x^4}\right)\frac{\partial^2\varphi}{\partial x^2} = 0, \qquad x > 0,$$
$$\gamma^2\varphi + \left(1 + \frac{h_2^3}{h_1^3}\frac{\partial^4}{\partial x^4}\right)\frac{\partial^2\varphi}{\partial x^2} = 0, \qquad x < 0. \tag{3.2}$$

Dispersion equation (2.7) in normalized variables (3.1) is given by

$$\gamma^2 = k^2(1 + k^4), \qquad x > 0;$$
$$\gamma^2 = k^2\left(1 + \frac{h_2^3}{h_1^3}k^4\right), \qquad x < 0, \tag{3.3}$$

where k is a dimensionless wavenumber.

The general solution to the problem (3.2) is presented by the linear combination of solutions (2.4) with arbitrary coefficients

$$\varphi = \sum_{j=1}^{6} \varphi_j^{(l)}\exp(ik_j^{(l)}x),$$
$$l = 1,\ x > 0; \qquad l = 2,\ x < 0, \tag{3.4}$$

where the numbers $k_2^l = -k_1^l$, $k_1^l > 0$ are real roots of dispersion equation (3.3), while k_3^l, $k_4^l = (k_3^l)^*$, $k_5^l =$

$-k_3^l$, and $k_6^l = -(k_3^l)^*$ are its complex roots. Velocity potential (3.4) is defined by 12 arbitrary constants $\varphi_j^{(l)}$, specified by asymptotic conditions as $|x| \to \infty$ for the waves bringing energy from infinity to the irregularity, by conservation laws and by the contact-boundary conditions at the proper irregularity.

The above asymptotics as $|x| \to \infty$ is given by two pairs of superposed real waves, two of them incident with amplitudes $\varphi_1^{(1)}$ and $\varphi_2^{(2)}$ bringing energy onto the irregularity and the other two (reflected with $\varphi_1^{(2)}$ and $\varphi_2^{(1)}$) taking energy away from there:

$$\varphi \sim \varphi_1^{(1)}\exp(i(k_1^{(1)}x + \gamma t)) + \varphi_2^{(1)}\exp(i(k_2^{(1)}x + \gamma t)), \quad x \to \infty,$$

$$\varphi \sim \varphi_1^{(2)}\exp(i(k_1^{(2)}x + \gamma t)) + \varphi_2^{(2)}\exp(i(k_2^{(2)}x + \gamma t)), \quad x \to -\infty,$$

$$\varphi_j^{(1)} = 0, \quad j = 4, 5; \quad \varphi_j^{(2)} = 0, \quad j = 3, 6. \tag{3.5}$$

The balance of energy fluxes directed to and from the irregularity, invoking (2.9), yields

$$c^{(1)}(|\varphi_1^{(1)}|^2 - |\varphi_2^{(1)}|^2) = c^{(2)}(|\varphi_1^{(2)}|^2 - |\varphi_2^{(2)}|^2),$$

$$c^{(l)} = \frac{\partial \gamma}{\partial k}, \quad k = k_1^{(l)}, \; l = 1, 2. \tag{3.6}$$

Then we can introduce the complex coefficients of wave reflection and transmission as

$$R_{11} = \frac{\varphi_2^{(1)}}{\varphi_1^{(1)}}, \qquad T_{12} = \frac{\varphi_1^{(2)}}{\varphi_1^{(1)}}\left(\frac{k_1^{(2)}}{k_1^{(1)}}\right)^2,$$

$$R_{22} = \frac{\varphi_1^{(2)}}{\varphi_2^{(2)}}, \qquad T_{21} = \frac{\varphi_2^{(1)}}{\varphi_2^{(2)}}\left(\frac{k_2^{(1)}}{k_2^{(2)}}\right)^2, \tag{3.7}$$

where R_{11} is the ratio between complex amplitudes of the wave coming from $x = +\infty$ and the backscattered wave, T_{12} is the ratio between the amplitudes of the waves outgoing to $x = -\infty$ and incident from $x = +\infty$. Coefficients R_{22} and T_{21} have similar physical meaning. (Recall that wave amplitude corresponds to the amplitude of fluid displacement above the equilibrium horizontal position.)

From (3.6) and (3.7), the reflection and transmission coefficients are related by Fresnel formulas

$$(k_1^{(1)})^2 c^{(2)}(1 - |R_{22}|^2) = (k_2^{(2)})^2 c^{(1)}|T_{21}|^2,$$

$$(k_2^{(2)})^2 c^{(1)}(1 - |R_{11}|^2) = (k_1^{(1)})^2 c^{(2)}|T_{12}|^2,$$

$$(k_2^{(2)})^2 c^{(1)}(R_{11}T_{21}^* + R_{11}^* T_{21}) + (k_1^{(1)})^2 c^{(2)}(R_{22}T_{12}^* + R_{22}^* T_{12}) = 0. \tag{3.8}$$

For instance, if the ice cover thickness is the same on the two sides of an irregularity, (3.8) reduces to

$$|R|^2 + |T|^2 = 1, \qquad \mathrm{RT}^* + TR^* = 0,$$

$$T_{12} = T_{21} = T, \qquad \mathrm{R}_{11} = R_{22} = R. \tag{3.9}$$

Let us consider Eq. (3.9) in the asymptotic case as $\gamma \to \infty$, which is formally beyond the shallow-water theory but is useful for understanding general features of the similar finite depth problems. At $D_2 > 0$ from the first equation in (3.9) we find

$$\sqrt{D_2}(1 - |R_{22}|^2) = |T_{21}|^2, \quad \gamma \to \infty, \tag{3.10}$$

whence $T_{21} \to 0$ as $D_2 \to 0$. In other words, the transmission of high-frequency flexural–gravity waves from an area covered with thin ice into a field of thick ice is close to zero. Actually, at $D_2 = 0$ we deduce from (3.9) that

$$1 - |R_{22}|^2 = 3\gamma^2|T_{21}|^2, \quad \gamma \to \infty. \tag{3.11}$$

Therefore, the elastic plate represents a rigid wall reflecting totally the incident high-frequency waves.

The second equation of set (3.9) reduces to

$$\sqrt{D_2}|T_{12}|^2 = (1 - |R_{11}|^2), \qquad \gamma \to \infty,$$

$$|T_{12}|^2 = 3\gamma^2(1 - |R_{11}|^2), \tag{3.12}$$

which cannot explain the asymptotics of wave transmission from thick ice to thin ice or to open water. In section 2 we showed that for two waves of equal energy the larger amplitude belongs to the wave propagating beneath the thinner ice. Hence, the amplitude of a wave passing from thick to thin ice can grow, in principle but not necessarily, because some energy transfers into the reflected wave. Thus, this problem should be solved in a complete diffractional formulation.

Before a numerical analysis, we rewrite the contact-boundary conditions, respectively, for a crack (2.12)

$$\lim_{x\to\pm 0}\frac{\partial^4\varphi}{\partial x^4} = 0, \qquad \lim_{x\to\pm 0}\frac{\partial^5\varphi}{\partial x^5} = 0 \tag{3.13}$$

and a hummock (2.14)

$$\mu\gamma^2\eta_0 + \lim_{x\to+0}\frac{\partial^3\eta}{\partial x^3} - \lim_{x\to-0}\frac{\partial^3\eta}{\partial x^3} = 0,$$

$$\mu_t\gamma^2\phi + \lim_{x\to+0}\frac{\partial^2\eta}{\partial x^2} - \lim_{x\to-0}\frac{\partial^2\eta}{\partial x^2} = 0,$$

$$\lim_{x\to\pm 0}\frac{\partial^2\eta}{\partial x^2} \pm \tilde{\alpha}\left(\lim_{x\to\pm 0}\frac{\partial\eta}{\partial x} + \phi\right), \quad \lim_{x\to\pm 0}\eta = \eta_0,$$

$$\mu = \frac{mH}{\rho l^3}, \qquad \mu_t = \frac{IH}{\rho l^5}, \qquad \tilde{\alpha} = \frac{\alpha}{\rho g l^3} \tag{3.14}$$

with the normalized parameters and angular variable

$$\Phi = \frac{a\phi}{l},$$

where a is a characteristic vertical displacement of the ice cover.

Further computations are conducted for the case when the wave of unit amplitude $\varphi_2^{(2)} = 1$ brings energy from the side $x = -\infty$ with no energy flux from the other

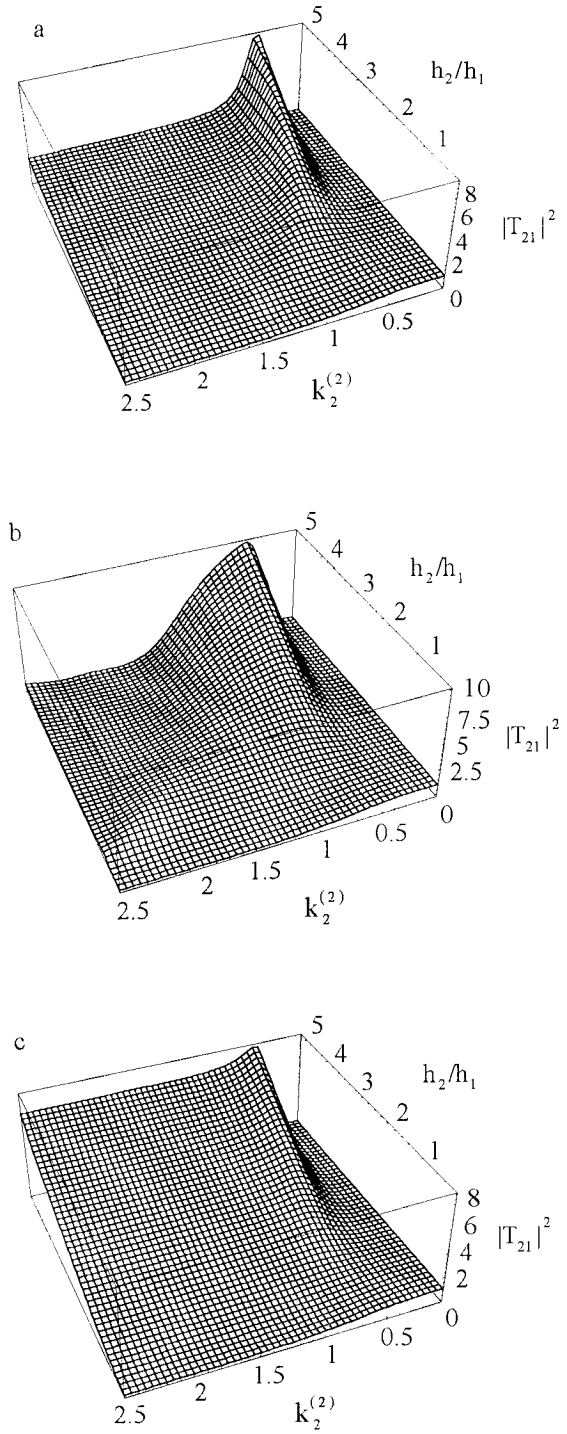

FIG. 3. Dependency of the squared modulus $|T_{21}|^2$ of wave transmission coefficient on the incident wavenumber $k_2^{(2)}$ and the ratio h_2/h_1 of ice thicknesses separated by the cover irregularity: (a) crack with free edges; (b) hummock with the reduced values of mass $\mu = 0.6$, moment of inertia $\mu_t = 0.05$, and rigidity of hinges $\tilde{\alpha} = 10^5$; and (c) crack with fused edges.

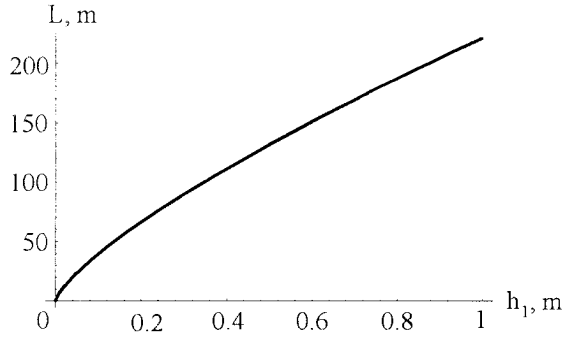

FIG. 4. Wavelength L of the incident wave with the highest transmission, depending on the ice thickness h_1.

side, $\varphi_1^{(1)} = 0$. For the diffraction at a hummock we take the numerical parameters $\mu = 0.6$ and $\mu_t = 0.05$ to correspond to estimates (2.2) and (2.13) if the fluid depth does not exceed $H = 100$ m and the hummock sail is on the order of the ice thickness, $h_r \leq 3$ m.

Some computations are also made for the limiting case of $\mu = \mu_t = \tilde{\alpha} = 0$—that is, for the ice crack with edges not displacing but rotating freely around the contact line. This is the case of compressed ice cover, where the relative displacement of the edges is hindered by friction; then the plate's motion should, in general, be affected by the vertical compressing force. A simple estimate shows that a vertical compression up to 10^6 N m^{-2} [ice strength by Bogorodsky and Gavrilo (1980)] is negligible compared to the effects of gravity and elasticity.

Figure 3 is a plot of the dependency of the squared modulus $|T_{21}|^2$ of the transmission coefficient, that is, transmission by wave energy, versus incident wavenumber $k_2^{(2)}$ and the ratio of ice thicknesses separated by the cover irregularity (this figure is for wave vectors within the range of the shallow water approximation). Wave diffraction at a crack with free edges is presented in Fig. 3a; the process at a hummock for $\tilde{\alpha} = 10^5$ is shown in Fig. 3b, and Fig. 3c corresponds to the diffraction at the crack with no relative displacement of edges.

The wave transmission through a crack with free edges (Fig. 3a) decreases monotonically as the wave vector $k_2^{(2)}$ grows at rather small ratio h_2/h_1. Beginning with a certain ratio less than unity, we see a local transmission maximum at $k_2^{(2)} \approx 0.5$, which is the greater at larger h_2/h_1. At $h_2/h_1 = 5$ the modulus of transmission coefficient reaches approximately 2.8. The shorter waves are more strongly reflected by the crack, in the relevant limit the amplitude of transmitted waves exceeding that of reflected ones, if the ratio h_2/h_1 is greater than some critical value above the unity.

The maximum amplification at $k_2^{(2)} = 0.5$ in dimensional parameters corresponds to wavelength $L = 4\pi l$, where the characteristic length l is determined by (3.1) through the ice rigidity and cover thickness. For clarity, the dependence of L on h_1 is plotted in Fig. 4 to show

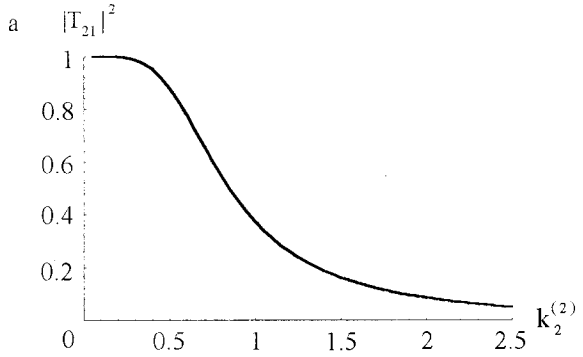

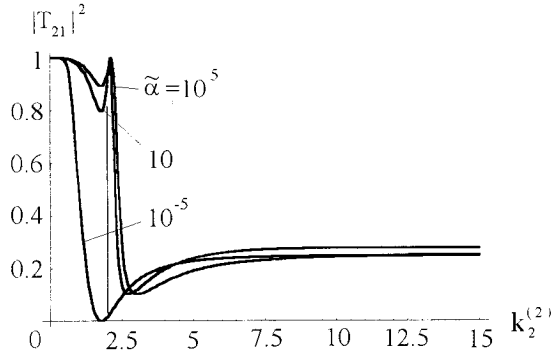

FIG. 6. Frequency dependency of the wave energy transmission $|T_{21}|^2$ through the ice ridge for various hinge elasticities $\tilde{\alpha}$.

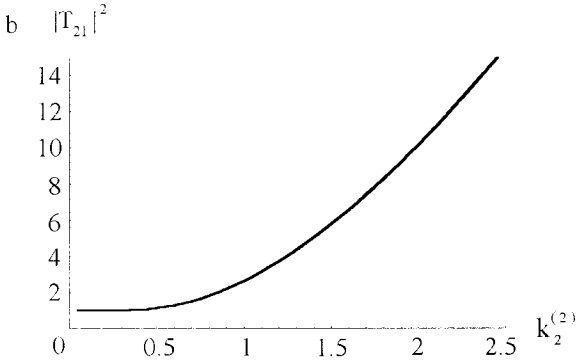

FIG. 5. Wave energy transmission $|T_{21}|^2$ in the shallow water limit for (a) the wave coming from the open water to the ice field and (b) in opposite direction.

that, for example, at $0.8 < h_1 < 1$ m, the length of the most penetrative wave is (on the crack's left side) about 200 m, thus corresponding to the shallow water approximation at fluid depth no more than 30 m. The transmitted wave is a little less than 150 m long.

As mentioned above, the short-wave asymptotics is outside of the shallow water approximation; however, it demonstrates the wave transmission qualitatively at arbitrary fluid depth. It is clear from qualitatively similar shallow water dispersion law (3.3) and relation $\gamma^2 = k(1 + Dk^4)\tanh(kH)$ for a fluid of finite depth H. The asymptotics of $\gamma(k)$ as $k \to \infty$ has powers 5/2 and 3, respectively, for finite depth and shallow water, and evidently coincides for small wave vectors. The group and phase velocities of short waves greatly exceed those of long waves in the two cases. At $D = 0$ the short wave velocities are much less than those of long ones at finite depth, but all wave velocities are the same in shallow water (as a function of depth).

Figures 5a and 5b present the shallow water dependencies $|T_{21}|^2(k_2^{(2)})$ in limiting cases $h_2 = 0$ and $h_2/h_1 = \infty$, corresponding respectively to the wave output from the open water to the ice field and vice versa. In the former case, the transmission vanishes for short waves, while in the latter it grows monotonically as $k_2^{(2)} \to \infty$. Thus, short-wave transmission is asymptotically the same for $h_2 = 0$ and $h_2 \to 0$, whereas it differs dramatically for the cases of $h_2 > 0$, $h_1 = 0$, and $h_2 \gg h_1 > 0$, which indicates a strong impact of ice cover of any thickness on the short waves. Therefore, the asymptotic wave transmission through a crack dividing thick and thin ice fields always differs from that as a short wave propagates from an area covered with ice into open water.

The dependency of $|T_{21}|^2$ on $k_2^{(2)}$ and h_2/h_1 on a hummock (Fig. 3b) is rather complicated. Some transmission features are the same as in the case of a crack with free edges: the local maximum at wavelength close to L and asymptotically zero transmission of short waves at $h_2 = 0$. This complex shape of the surface $|T_{21}(k_2^{(2)}, h_2/h_1)|^2$, as in Fig. 3b, is due to interaction of rotational and vertical (heave) modes of the hummock motion. The wave diffraction by a hummock frozen within a homogeneous ice plate is illustrated in Fig. 6 for various parameters $\tilde{\alpha}$ of coupling between the hummock and the plate. The main common feature there is the point $k_2^{(2)} \approx 2$ of almost the total transmission, depending but slightly on $\tilde{\alpha}$. (Even the curve with $\tilde{\alpha} = 10^{-5}$ shows the unit transmission there, designated in Fig. 6 by a thin vertical line.) It is noteworthy that the above peculiarity is only probable since it lies somewhere at the edge of the range of applicability for shallow water theory.

The dependency of transmission on the wave vector and the ratio of ice thicknesses for a crack with fused edges is qualitatively similar to that for a crack with free edges, differing only for short waves more strongly reflected by free edges. Physically, it is quite clear because the plate-free edges present a greater inhomogeneity than adhered ones.

It is noteworthy that in all the three cases illustrated by Fig. 3 the local maximum of transmission is near the wave vector $k_2^{(2)} = 0.5$. This value is characteristic of the reflecting effect for the thin ice. For comparatively long incident waves and $h_2 > h_1$, the wave transmission

through an irregularity is qualitatively similar to the output from the ice field to the open water.

4. Diffraction at several cracks

Let the fluid motion be caused by a flexural–gravity wave of unit amplitude with the wave vector k, incident from $x = -\infty$ onto N irregularities. The complex amplitudes of waves reflected R_{N-1} and transmitted T_{N-1} through the $N - 1$th irregularity are known and the spacing between $N - 1$th and Nth irregularities is l_{N-1}. The irregularities lie along the straight lines $x = a_j$, $j = 1 - N - 1$; $a_1, a_2, \cdots, a_{N-1}$. By virtue of linearity of the problem, interactions of the wave with each irregularity are independent. Therefore the amplitudes of waves reflected R_N and transmitted T_N by N irregularities of the same type are presented by the series:

$$R_N = R_{N-1} + (T_{N-1})^2 e^{2ikl_{N-1}} R_1 (1 + R_1 R_{N-1} e^{2ikl_{N-1}} + (R_1 R_{N-1} e^{2ikl_{N-1}})^2 + \cdots),$$

$$T_N = T_{N-1} T_1 e^{ikl_{N-1}} [1 + R_1 R_{N-1} e^{2ikl_{N-1}} + (R_1 R_{N-1} e^{2ikl_{N-1}})^2 + \cdots]. \quad (4.1)$$

Calculating the sums of geometric progressions, we find

$$R_N = R_{N-1} + \frac{(T_{N-1})^2 e^{2ikl_{N-1}} R_1}{1 - R_1 R_{N-1} e^{2ikl_{N-1}}},$$

$$T_N = \frac{T_{N-1} T_1 e^{ikl_{N-1}}}{1 - R_1 R_{N-1} e^{2ikl_{N-1}}}. \quad (4.2)$$

For two of the same irregularities spaced by distance l_1, we have respectively

$$R_2 = R_1 + \frac{R_1 (T_1)^2 e^{2ikl_1}}{1 - (R_1)^2 e^{2ikl_1}},$$

$$T_2 = \frac{(T_1)^2 e^{ikl_1}}{1 - (R_1)^2 e^{2ikl_1}}. \quad (4.3)$$

As mentioned, at rather high frequencies the coefficients R_1 and T_1 are virtually constant. In this case it follows from (4.3) that R_2 and T_2 depend on k quasiperiodically with amplitude of the oscillations close to unity. In other words, a countable set of frequencies exists with $k = n\pi - \arg(R_1)$, $n = 0, \pm 1, \pm 2, \cdots$, at which the waves pass the system of two irregularities without energy loss. Physically it is quite clear because some resonant (Bragg type) wave scattering is observed at the crack grating in the frequency range where the wave transmission through a single crack is independent of frequency.

The dispersion of transmission coefficient for two cracks, $|T_2(k)|^2$, is presented in Fig. 7a, where their spacing is chosen as a scale and the normalized ice plate rigidity is $D = 10^{-2}$. For elasticity $E = 10^{10}$ N m^{-2} and ice thickness $h = 2$ m, the scale is $l \approx 94$ m; that is, the dimensional wave vector is $k/94$ m^{-1}. One sees that at $k > 2$ the wave transmission becomes quasiperiodic with narrow unit maxima, while the wave vector intervals with minimum transmission are wider, excluding the range of long waves with almost the total transmission.

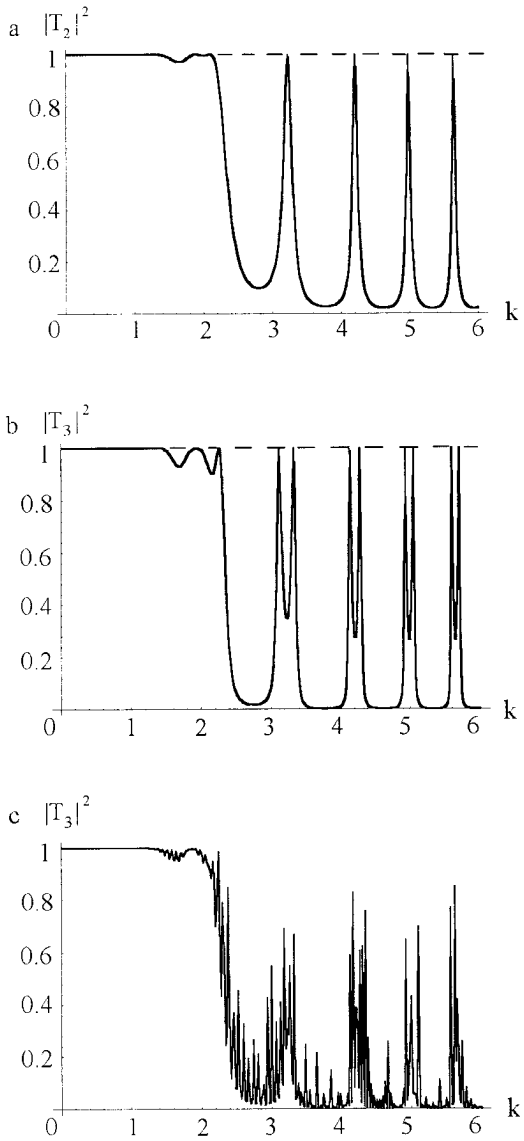

FIG. 7. Wavenumber dependency of the wave transmission through two (a) and three cracks with free edges in the ice cover with (b) equal and (c) strongly different (1:20) spacing between them.

The dependency $|T_3(k)|^2$ for the wave diffraction at three equidistant cracks is plotted in Fig. 7b at the above ice cover parameters. The general run of this function is quite similar to that for two cracks. However, in a small vicinity of each local maximum of $|T_2(k)|^2$, there are two maxima of $|T_3(k)|^2$, and the minimum of $|T_3(k)|^2$ is less than that of $|T_2(k)|^2$.

In a general case of N irregularities arranged through the same spacing, relations (4.2) give also the periodic dependence of R_N and T_N on k at high frequencies. But, if the distances between irregularities differ, then the high-frequency wave coefficients R_N and T_N are expressed via products of periodic functions with incommensurable periods. Therefore, the coefficients should have numerous local extrema with varying distances between them. A typical example is shown in Fig. 7c for three cracks, where the distance between the second and third cracks exceeds that between the first and second by a factor of 20.

It seems that as $N \to \infty$, one can only consider the probability of the wave passing through an infinite number of irregularities with random spacing because in any vicinity of a wave vector with nonzero transmission a point k with total reflection exists. If the spacing between irregularities is constant, the frequency dependencies of reflection and transmission should contain forbidden gaps of zero transmission and allowed zones of total transmission. We consider these effects in more detail next.

5. Diffraction at a periodic system of inhomogeneities in the ice cover

We analyze two types of periodically inhomogeneous ice cover. In the first case it is supposed that the ice plate is discontinuous but consists of ice bands with finely broken ice floating in between. In the second case we assume the ice cover contains an infinite number of rectilinear, parallel, and equidistant hummock ridges. We will try to determine the conditions under which undamped surface waves exist.

Let us employ the dimensionless variables (3.1), taking the period of irregularity in the ice cover as a characteristic horizontal scale l. The equations of motion are then reduced to the system of the type of (3.2) with

$$\gamma^2\varphi + \left(1 + D\frac{\partial^4}{\partial x^4}\right)\frac{\partial^2\varphi}{\partial x^2} = 0, \tag{5.1}$$

where

$$D = \frac{Eh^3}{12\rho g(1 - \nu^2)l^4}$$

in the ice bands and $D = 0$ in the areas filled by finely broken floating ice.

In order to solve the problem in the case of bands, we must determine the conditions under which (3.2) has bounded traveling-wave solutions satisfying an infinite number of the contact-boundary conditions on the floe edges

$$\frac{\partial^4\varphi}{\partial x^4} = 0, \qquad \frac{\partial^5\varphi}{\partial x^5} = 0,$$
$$x \to j + 0, \qquad x \to J + N - 0,$$
$$j = 0, \pm 1, \pm 2, \cdots \tag{5.2}$$

and conservation laws for energy and momentum

$$[\varphi] = 0, \qquad [\partial\varphi/\partial x] = 0,$$
$$x = \mathrm{j}, \qquad x = j + N. \tag{5.3}$$

Note that one spatial period takes the interval $j < x < j + N$, where N characterizes the ice concentration on the fluid surface and is an analogue of the ice cover compactness.

In the second case of floating broken ice, the contact-boundary conditions and conservation laws are given by

$$D\left(\lim_{x\to j+0}\frac{\partial^3\eta}{\partial x^3} - \lim_{x\to j-0}\frac{\partial^3\eta}{\partial x^3}\right) - \mu\gamma^2 \lim_{x;\ \mathrm{raj}+0}\eta = 0,$$
$$(\tilde\alpha - \mu_t\gamma^2 D)\lim_{x\to j-0}\frac{\partial^2\eta}{\partial x^2} - \tilde\alpha \lim_{x\to j+0}\frac{\partial^2\eta}{\partial x^2} - \tilde\alpha\mu_t\gamma^2 \lim_{x\to j-0}\frac{\partial\eta}{\partial x} = 0,$$
$$(\tilde\alpha - \mu_t\gamma^2 D)\lim_{x\to j+0}\frac{\partial^2\eta}{\partial x^2} - \tilde\alpha \lim_{x\to j-0}\frac{\partial^2\eta}{\partial x^2} - \tilde\alpha\mu_t\gamma^2 \lim_{x\to j+0}\frac{\partial\eta}{\partial x} = 0,$$
$$\lim_{x\to j+0}\eta = \lim_{x\to j-0}\eta, \qquad [\varphi] = \left[\frac{\partial\varphi}{\partial x}\right] = 0, \qquad x = j. \tag{5.4}$$

Solution of these problems reduces to finding the eigenvalues of the monodromic matrix. The intervals of frequency γ in which the modulus of each eigenvalue is not equal to unity are the forbidden gaps. Waves whose frequencies belong to forbidden gaps cannot propagate undamped beneath the inhomogeneous ice. If the wave frequency lies outside the forbidden zones, then the equations have bounded solutions that are periodic functions of time. These solutions correspond to waves that propagate without energy loss.

Let us construct the monodromic matrix for the case of broken ice cover. Within the interval $x \in (j, j + 1)$, the solution for the wave amplitudes can be written as

$$\varphi = C_1^j\varphi_1^j + C_2^j\varphi_2^j,$$
$$\varphi_r^j = e^{ik_r(x-j)} + \sum_{l=3}^{6} C_{rl}e^{ik_l(x-j)},$$
$$x \in (j, j + N),$$
$$\varphi_r^j = C_{+r}^j e^{i\gamma(x-j)} + C_{-r}^j e^{-i\gamma(x-j)},$$
$$x \in (j + N, j + 1),\ r = 1, 2,$$

where the wavenumbers $k_{1,2}$ and k_{3-6} are the real and

complex roots of the dispersion equation $\gamma^2 = k^2(1 + Dk^4)$. The constants $C^j_{\pm r}$ and C_{rl} satisfy a system of linear algebraic equations, which follow from the contact-boundary conditions (5.4):

$$k_r^4 + \sum_{l=3}^{6} C_{rl}k_l^4 = 0, \qquad k_r^5 + \sum_{l=3}^{6} C_{rl}k_l^5 = 0,$$

$$k_r^4 e^{ik_rN} + \sum_{l=3}^{6} C_{rl}k_l^4 e^{ik_lN} = 0,$$

$$k_r^5 e^{ik_rN} + \sum_{l=3}^{6} C_{rl}k_l^5 e^{ik_lN} = 0,$$

$$k_r e^{ik_rN} \sum_{l=3}^{6} C_{rl}k_l e^{ik_lN} = \gamma(C_{+r}e^{i\gamma N} - C_{-r}e^{-i\gamma N}),$$

$$e^{ik_rN} + \sum_{l=3}^{6} C_{rl}e^{ik_lN} = C_{+r}e^{i\gamma N} + C_{-r}e^{-i\gamma N}.$$

Let the solution in the interval $x \in (j, j + 1)$ be equal to φ_r^j. The constants C_r^{j+1} are found from the conditions (5.3) at the points $x = j$,

$$C_{+r}e^{i\gamma} + C_{-r}e^{-i\gamma} = C_1^{j+1}\left(1 + \sum_{l=3}^{6} C_{1l}\right) + C_2^{j+1}\left(1 + \sum_{l=3}^{6} C_{2l}\right),$$

$$\gamma(C_{+r}e^{i\gamma} - C_{-r}e^{-i\gamma}) = C_1^{j+1}\left(k_1 + \sum_{l=3}^{6} k_l C_{1l}\right) + C_2^{j+1}\left(k_2 + \sum_{l=3}^{6} k_l C_{2l}\right). \quad (5.5)$$

Equations (5.5) have solutions corresponding to $r = 1$ and $r = 2$. The monodromic matrix has the form

$$\mathbf{T} = \begin{pmatrix} C_1^{j+1}\big|_{r=1} & C_2^{j+1}\big|_{r=1} \\ C_1^{j+1}\big|_{r=2} & C_2^{j+1}\big|_{r=2} \end{pmatrix}.$$

We pass to another basis in the space of functions φ_r^j in which $\mathbf{T}$ is a diagonal matrix. An arbitrary solution in the new basis is a superposition of new basis functions ψ_r^j. In this basis, the elements of $\mathbf{T}$ are its eigenvalues T_r. The solution $\psi_r^{j+1}(x_0)$, where $x_0 \in (j + 1, j + 2)$, is equal to the product $T_r\psi_r^j(x_0 - j)$. This shows that if the absolute eigenvalue of the matrix is not unity, then the wave exponentially decays in one direction or grows in the other.

The monodromic matrix $\mathbf{T}$ for an ice cover with a periodic system of hummocks is constructed in a similar way. The solution is represented in the form

$$\varphi = \sum_{l=1}^{6} C_l^j e^{ik_l(x-j)}, \qquad x \in (j, j + 1),$$

where the constants C_k^{j+1} are related to C_l^j via (5.4). The

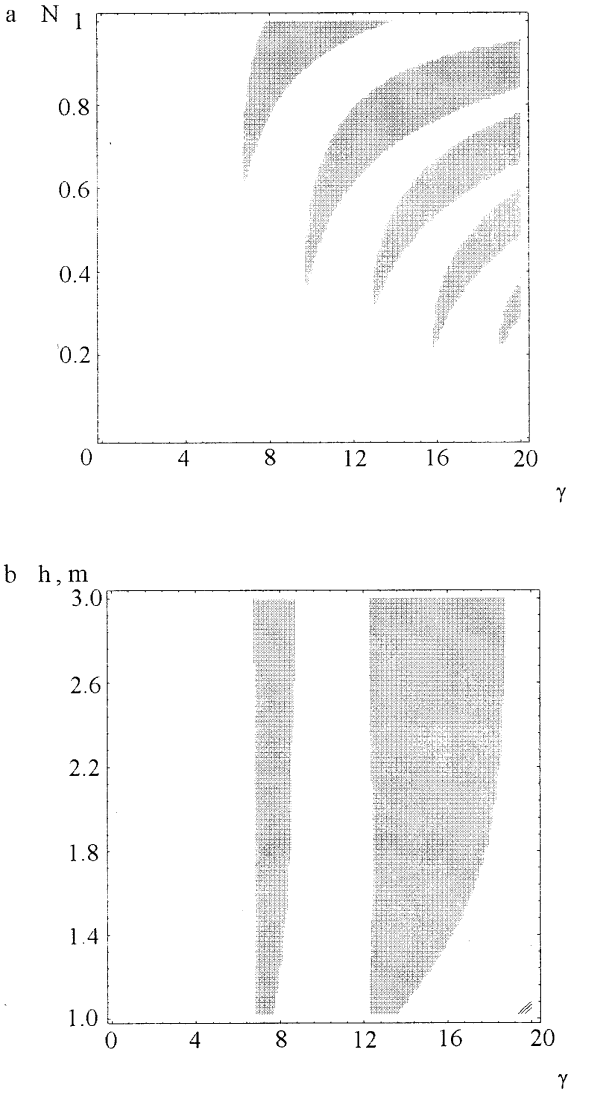

FIG. 8. Forbidden gaps for the wave propagation in a broken ice: the ordinate axis corresponds to (a) the relative ice concentration N and (b) the ice thickness h for the concentration $N = 0.8$. The abscissa is the dimensionless wave frequency γ.

nth row of $\mathbf{T}$ (which is a 6×6 matrix) is a solution to (5.4) in terms of C_k^{j+1} for $C_k^j = 0$, $k \neq n$, $C_n^j = 1$. The eigenvalues of the monodromic matrix are functions of the frequency γ and the ice cover parameters N, D, μ, μ_t, and $\tilde{\alpha}$.

Numerical calculations were carried out for a fixed l and various values of γ, N, h, and h_r. The hummock parameters μ and μ_t were determined by (2.14) and (3.11). The calculated data are shown in Figs. 8 and 9 in the parameter planes (γ, N), (γ, h), (γ, h_r). Thus, when each point is calculated, all parameters are fixed except the fluid depth H, which enters the definition of dimensional frequency $\omega = \gamma\sqrt{gH}/l$. Therefore, the interpretation of these data in dimensional variables depends on the depth H.

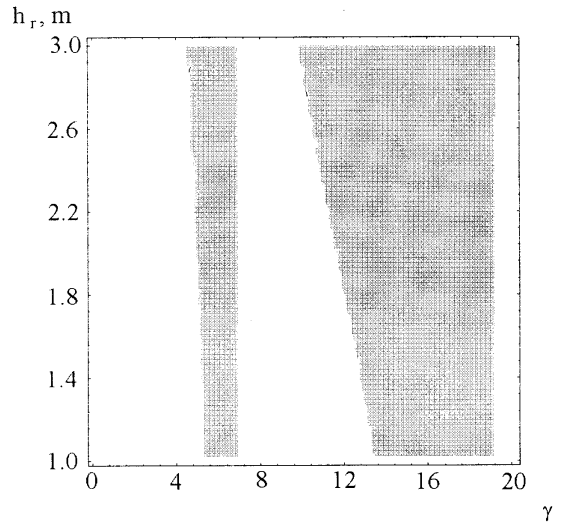

FIG. 9. Forbidden gaps for the wave propagation in a hummocked ice: dependency of the ridge sail on dimensionless wave frequency γ.

The fluid and ice parameter values were typical for shelf areas of the Russian Arctic seas. The depth H was varied from 10 to 50 m. The Young module, Poisson's ratio, and ice density were determined by (2.2). The ice thickness and the hummock sail were varied from 1 to 3 m. Because the hummocks usually arise at the places of contact between floes, the distance between adjacent hummocks was assumed to be on the order of the floe size. The characteristic horizontal scale l was set to 100 m. (At a smaller scale the shallow water equations are invalid, while for $l \gg 100$ m the ice cover virtually does not interact with the surface wave.) The dimensionless coefficient $\tilde{\alpha}$ of the hummock coupling with ice was taken to be 10^{-5}. The dimensional quantity α is produced by multiplying the latter by $\rho g l^3 \geq 10^{10}$ N. For a hummock rigidly fixed to the ice cover, $\alpha = \infty$, and for floe edges rotating freely around the hummock, $\alpha = 0$. Thus, the value of $\tilde{\alpha}$ used in the calculations corresponds to the hummock weakly attached to the ice.

The forbidden gaps in the wave frequency spectrum are shown in Fig. 8 by gray shading. Typical examples of forbidden gaps for waves in broken ice are plotted in Figs. 8a,b. The dimensionless frequency γ lies along the horizontal axes. In Fig. 8a the vertical axis is the concentration parameter N for $h = 2$ m. The frequency spectrum displays forbidden gaps at $N > 0.2$. With growing N these zones become wider, and the boundary of the first gap shifts toward lower frequencies down to $\gamma_1 \approx 7$. Let us suppose that surface wave packets of various spectral composition propagate under an ice cover that has extended fields of different tightness. Then scattering by these irregularities should lead to an exponential attenuation of all waves whose dimensionless frequencies are greater than 7. The dimensional frequency ω_1 corresponding to γ_1 varies from 0.7 to 1.5 s^{-1} as H varies from 10 to 50 m, and embraces wave periods from 4.2 to 9 s.

Figure 8b shows the forbidden gaps at ice concentration $N = 0.8$. The ice cover thickness in meters is plotted along the vertical axis. The forbidden gaps become wider with growing ice thickness, their left-hand boundary remaining virtually the same.

Typical forbidden gaps for a hummocked ice cover are shown in Fig. 9 for $h = 1$ m. The dimensionless frequency γ is plotted along the horizontal axis in the same range as in Figs. 7a,b. Along the vertical the hummock sail h_r is plotted in meters. As this sail and, hence also, the hummock mass increase, the forbidden gaps widen with no virtual change in their right-hand boundary. Calculations show that at wave passage through hummocked ices the boundary of the first gap can shift toward lower frequencies down to $\gamma = 4$. In dimensional variables, this boundary can lie in the frequency range $0.4 < \omega_2 < 0.9$ s^{-1} for sea depth H varying from 10 to 50 m, that is, period of waves with relevant frequency in the interval from 16 to 7 s.

6. Conclusions

We have studied the interaction of flexural–gravity waves propagating at the surface in shallow water beneath an elastic ice cover with linear irregularities modeling cracks and hummocks. In all the cases considered the transmission coefficient tends to unity as the wavelength tends to infinity. Physically this means a weak impact of ice cover on propagating long waves.

When passing a single irregularity, the wave energy is partly reflected and transmitted. If the ice thickness has a discontinuity there, then the amplitude of passed wave can exceed that of the incident one. An extreme increase of wave amplitude occurs when the dimensionless wavenumber is close to 0.5. For instance, if the ice thickness is 1 m, then such a value corresponds to wavelengths of about 200 m.

For wave diffraction on a finite set of the ice cover irregularities with the same spacing, the transmission depends periodically on wavenumber for sufficiently short incident waves. There are a countable set of wavenumbers at which the transmission coefficient is equal to unity in absolute value and the waves pass totally through the irregularity. Another countable set of wavenumbers has the transmission close to zero. These local minima are rather smooth so that waves with numbers in the vicinity of the minima are strongly reflected by periodic irregularities.

For different spacing between adjacent irregularities, the transmission dependency on wavelength is sharply stepped. There are local maxima in small vicinities of local minima; therefore the scattering of waves with close frequencies can proceed with different scenarios.

If an infinite set of irregularities is periodically distributed over ice cover of permanent thickness, the frequency spectrum has forbidden gaps where the incident waves are totally scattered by the irregular ice cover and attenuate exponentially when propagating under it. The first forbidden gap is separate from the zero frequency, and very long waves travel beneath the ice with small energy loss. Meanwhile, the gap can contain the frequencies of typical swells and wind waves, which should be strongly scattered by the irregular ice cover. This pattern agrees with the experimental observations in the Arctic by Wadhams and Wells (1995), who measured only the low-frequency part of swells propagating under the ice from open water.

In the case of a large number of irregularities arranged randomly over the ice cover, one could probably speak only about a probable existence of an undamped flexural–gravity wave with specified period. Therewith, the probability of surviving low-frequency waves is close to unity. If the system of irregularities is nearly periodic, the probability reproduces the structure of forbidden gaps; that is, the probability of an undamped wave is almost zero in the vicinity of these gaps for the periodic problem.

It must be pointed out that all of the above results were derived for the shallow water approximation and are directly applicable only to shelf areas of the ocean.

Acknowledgments. This work was supported by the International Science Foundation jointly with the Russian government (Grants MFE300 and JJ4100) and by the Russian Foundation for Basic Research (Project Codes 93-02-16203 and 96-02-00252a).

REFERENCES

Bogorodsky, V. V., and V. P. Gavrilo, 1980: *Ice: Physical Properties. Modern Methods in Glaciology* (in Russian). Gidrometeoizdat, 384 pp.

Evans, D. V., and T. V. Davies, 1968: Wave–ice interaction. Davidson Laboratory, Stevens Institute Technology Rep. 1313, Hoboken, NJ, 102 pp.

Fox, C., and V. A. Squire, 1994: On the oblique reflection and transmission of ocean waves from shore fast sea ice. *Philos. Trans. Roy. Soc. London,* **A347**(1682), 185–218.

Kouzov, D. P., 1963: Plane hydroacoustic wave diffraction at a crack in an elastic plate. *Prikl. Mat. Mekh.,* **27**(6), 1037–1043.

Marchenko, A. V., 1994: Formation of flexural-gravity waves in the sea beneath ice cover. (*BRAS Physics*/*Supplement*) *Phys. Vibrations,* **58**(3), 220–235.

——, 1995: Natural vibrations of hummock ridge in an elastic ice sheet, floating on the surface of deep water. *Mekh. Zhidk. Gaza,* **6,** 99–105.

——, R. Purini, and K. I. Voliak, 1995: Filtering surface waves by ice floes. *Proc. POAC'95,* Vol. 3, Murmansk, Russia, Murmansk Shipping Company, 134–142.

Masson, D., and P. H. LeBlond, 1989: Spectral evolution of wind-generated gravity waves in a dispersed ice field. *J. Fluid Mech.,* **202,** 43–81.

Meylan, M., and V. A. Squire, 1994: The response of ice floes to ocean waves. *J. Geophys. Res.,* **99**(C1), 891–900.

Nagurny, A. P., V. G. Korostelev, and V. P. Abaza, 1994: Wave method for evaluating the effective thickness of sea ice in climate monitoring. (*BRAS Physics*/*Supple*), *Phys. Vibrations,* **58**(3), 168–174.

Smirnov, G. N., 1987: *Oceanography* (in Russian). Vysshaya Shkola, 407 pp.

Squire, V. A., J. P. Dugan, P. Wadhams, P. J. Rottier, and A. K. Liu, 1995: On ocean waves and sea ice. *Annu. Rev. Fluid Mech.,* **27,** 115–168.

Wadhams, P., and S. C. S Wells, 1995: Ice surface oscillation measurements on SIMI using strain, heave and tilt sensors. *Proc. Sea Ice Mechanics and Arctic Modeling Workshop,* Anchorage, AK, Office of Naval Research, 176–189.

Zubov, N. N., 1943: *Arctic Ice.* Izdatel'stvo Glavsevmorputi, 360 pp. (English translation, AD 426 972, U.S. Nav. Oceanogr. Office, NTIS, 5285 Port Royal Rd.,Springfield, VA 22161.)